energies

MDPI

Article

Energy Efficiency Analysis of Copper Ore Ball Mill Drive Systems

Piotr Bortnowski, Lech Gładysiewicz, Robert Król and Maksymilian Ozdoba *

Department of Mining and Geodesy, Faculty of Geoengineering, Mining and Geology, Wroclaw University of Science and Technology, 50-421 Wroclaw, Poland; piotr.bortnowski@pwr.edu.pl (P.B.); lech.gladysiewicz@pwr.edu.pl (L.G.); robert.krol@pwr.edu.pl (R.K.)
* Correspondence: maksymilian.ozdoba@pwr.edu.pl

Abstract: Milling is among the most energy-consuming technological stages of copper ore processing. It is performed in mills, which are machines of high rotational masses. The start of a mill filled to capacity requires appropriate solutions that mitigate the overloading. One method for increasing the energy efficiency of ball mills is to optimize their drive systems. This article looks at two variants of drive systems with efficiencies higher than the already existing solutions. The first variant is a low-speed synchronous motor with permanent magnets without a gearbox, and the second variant is an asynchronous high-efficiency motor with a gearbox and a fluid coupling. The energy performance analysis of the three solutions was based on the average energy consumption indicator per mass unit of the milled material and on the energy consumption per hour. The investigations required models of the drive systems and analyses with the use of the Monte Carlo methods. The highest energy efficiency is observed in the case of the solution based on the permanent magnet motor. However, the drive system with the high-speed motor offers a gentle start-up possibility owing to the fluid coupling.

Keywords: fluid coupling; ball mill; electric motor; drive system; grinding; energetic efficiency

Citation: Bortnowski, P.; Gładysiewicz, L.; Król, R.; Ozdoba, M. Energy Efficiency Analysis of Copper Ore Ball Mill Drive Systems. *Energies* **2021**, *14*, 1786. https://doi.org/10.3390/en14061786

Academic Editor: Sergey Zhironkin

Received: 26 February 2021
Accepted: 19 March 2021
Published: 23 March 2021

1. Introduction

Ore beneficiation and processing plants are among the biggest industrial facilities with respect to energy consumption. Therefore, research in this sector has been naturally focused on maximizing the energy efficiency. Energy efficiency is defined as an optimal (profitable) usage of energy for the purposes of current production or services. As the majority of this industrial sector uses highly-emissive sources of electric energy, the energy efficiency has in this case become an important point on the European Union's agenda [1]. A policy based on limiting the energy consumption is also an effective method for improving the competitiveness of an industrial plant and for maintaining constant technological progress, while reducing CO_2 emissions to the environment [2]. The first stage in the processing of raw materials (i.e., comminution) is the most energy-consuming, and accounts for up to 4% of global electric energy consumption [3–6]. In the United States, the milling process is estimated to account for 0.5% of the primary energy consumption, 3.8% of the total electric energy consumption, and 40% of the total energy consumption in the mining industry [7]. In Poland, the annual electric energy consumption from copper ore processing plants is approximately 2.5 TWh [8]. Primary ore comminution is performed with jaw and hammer crushers. Ore is then transferred to ball mills, in which it is first subjected to coarse grinding, and in the second phase (i.e., fine grinding) it is treated with grinding bodies (rods or cylpebs), which are introduced into the mill. Specific energy consumption during the milling process depends on the geomechanical parameters of the raw material and on the design parameters of the mill [9,10]. The energy demand indicator increases exponentially together with the decrease of the required grain size [11]. The cost of the energy used in comminution represents 50 ÷ 60% of the entire ore processing costs [12]. The above reason explains the importance of the research into new solutions for improving the energy efficiency of the comminution process.

2. Directions for Ore Processing Optimization

The literature mentions a number of examples of optimization-focused activities based on modeling the phenomena that occur during the milling process. Numerical simulation methods allow detailed analyses of the behavior of the material in the mill. For example, a previous publication [13] described a simulated model of a tumbling ball mill that allowed a number of operating recommendations to be formulated in order to increase the milling efficiency. In another example of the application of advanced numerical techniques, the authors of a previous study [14] used the ANSYS Fluent (manufacturer Ansys, Inc., Canonsburg, PA, USA) package to analyze a model of multiphase flow in a ball mill. The results of their research allowed a precise prediction of the flow with the free surface of the slurry in the mill.

Other optimization methods are based on the modernization of the milling process or on modifications of the mill design. If an adequate mill type is chosen for each milling stage already while designing the entire technological system, the total energy efficiency of the milling process is significantly influenced. Ball mills are applicable only in the primary milling. The milling efficiency and the related energy demand render impossible the use of ball mills for fine milling [15,16]. The number and the type of internal mill components (i.e., the type of the inner lining, the type and number of the diaphragms) are important for increasing the efficiency of the milling process, and this in turn translates directly into increased energy efficiency [17]. Mills with drum diameters greater than 5.5 m show lower energy efficiency at an optimal fill level of 40% [18]. The grinding media—their type and size—are also of significance [19]. The ratio between the size of the grinding media and the size of the comminuted particles is especially important. Research performed on this aspect demonstrates that the size of the particles in the mill feed significantly influences the energy efficiency of the comminution process, and by using an optimal crusher at the beginning of the technological system, this efficiency may be increased by as much as 10%. Wet milling significantly increases the energy consumption [20]. Specific energy demand by a mill depends on its efficiency, which is directly related to the speed of the mill. Optimal mill speed is typically 65 ÷ 75% of its critical speed, at which the milling process is no longer observed. In industrial conditions, mill speed can be regulated, for example, with the use of systems based on programmable logic controllers (PLCs) [21]. In the future, an important aspect of energy optimization may involve the concept of a single technological system incorporating devices that allow automation, as well as the processing and exchanging of data (Industry 4.0) for the purpose of monitoring the working conditions and controlling the parameters of the mill.

In another approach, the energy efficiency of milling may be improved by adjusting the parameters of the comminuted material with the use of chemical additives or water. Chemical additives may, however, have a negative environmental impact [22].

Energy savings may also be found in the ball mill drive systems. In the scale of a processing plant, the electric motors of these drive systems account for 95% of the total electric energy demand [23]. Therefore, the type of the motor used has a significant influence on the efficiency of the drive system. One of the solutions aimed at improving this efficiency is to use synchronous motors induced with permanent magnets. Motors of this type have a very high efficiency [24–26], and therefore they were used, in a low-speed version, in the modernized copper ore processing plant [27–29]. However, their operation entails a number of problems. Although low-speed motors eliminate the need to use a gearbox in the drive system, their start-up is rapid, which can damage its internal components and cause the overloading of the power supply line [30].

3. Analysis of Variant Ball Mill Drive Systems

The basic element of a ball mill is the drum, in which the milling process takes place (Figure 1). The length of the drum in the analyzed mill (without the lining) is 3.6 m, and the internal diameter is 3.4 m. The mass of the drum without the grinding media is 84 Mg. The drum is set in rotational motion by driving a ring gear mounted on the drive side. The

ring gear is engaged with a pinion gear. In versions with low-speed motors, the pinion is set on a shaft directly connected to the motor, and in versions with high-speed motors the pinion is set on an output shaft of the gearbox. The nominal mill efficiency, at optimum speed, is 80 Mg/h. The dimensions and the high mass of the rotating elements cause the drive system to be overloaded when the mill filled with copper ore is started. For this reason, the mill is stopped only in the case of a failure or planned maintenance work. The aim is to minimize the potential number of start-ups, as the mill at a standstill must be later started under full load. In the case of a prolonged downtime, the moist ore inside the mill hardens. During start-up, the mass is thus unevenly distributed with respect to the rotational axis of the mill. This condition is similar to the state of unbalance. This phenomenon causes unfavorable dynamic reactions in the mill bearings and excessive loads in other components of the drive system. Such conditions facilitate increased friction in the system, as well as noise emissions. They also increase the risk of damage to the motor itself, its overheating, or overloading of the power supply line [31–33].

Figure 1. Ball mill of the primary milling stage with the visible gear ring.

3.1. Traditional Drive System with SAS Motors

Designed already at the end of the twentieth century, the investigated drive systems of the ball mills installed in the copper ore processing plant were provided with SAS motors (Figure 2). The motors are synchronized in steady motion and powered from a 6 kV grid. Depending on the mill type, the power range of the SAS motors was 400 kW to 1120 kW. Low-power units work with 187.5 RPM, while higher-power units work with 166.6 RPM. Owing to this solution, the ball mill drive system does not have a gearbox [34].

(**a**) (**b**)

Figure 2. Ball mill drive system with low-speed SAS motor without intermediate gearbox: (**a**) prior to modernization, (**b**) after modernization on the right [34].

The nominal efficiency of the SAS motors, as declared by the manufacturer, is between 90% and 93%. Because they were manufactured in the 1970s, their efficiency after several decades in operation is estimated to have been reduced to 85%. Their compact design makes SAS motors particularly prone to the influence of an adverse, aggressive working environment. The most common operating problems experienced in motors of this type include rotor seizure or insulation damage due to moisture from the wet ore. The renovation cost of a single motor exceeds 25,000 USD.

Measurements of the current parameters with the use of the HIOKI loggers (HIOKI 9625, HIOKI E.E. CORPORATION, Nagano, Japan) show that the power consumed by the SAS motor in steady motion varies around a mean value of 602 kW (Figure 3). The rated power of this motor is 630 kW.

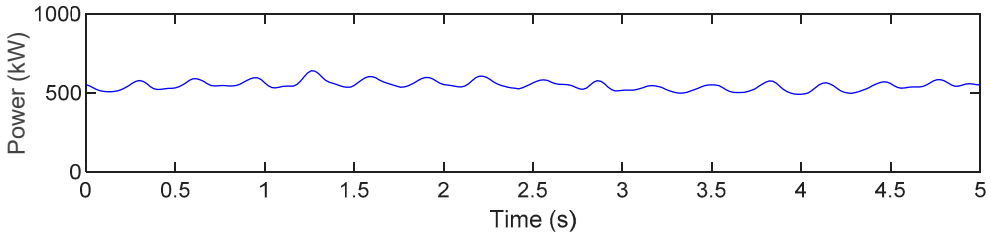

Figure 3. Active power of the SAS 630 kW motor during normal operation with filled ball mill.

Because of low efficiency and increasing maintenance costs, a decision was made to look for new solutions that would improve the energy efficiency [34].

3.2. The Drive System with a Low-Speed Motor Type LSPMSM SMH-1732T

One of the solutions aimed at increasing the energy efficiency of the milling process is to use new, energy-saving motors. The prototype drive system is based on a low-speed synchronous LSPMSM SMH-1732T motor (Figure 4), induced with permanent magnets. The design of the motor allows it to be directly connected to the power grid. The electric machine works in a three-phase system, with a supply voltage of 6 kV. The nominal power of the motor is 630 kW, and its most important advantage lies in its high efficiency, which is up to 97% [28,35]. The prototype LSPMSM motor replaced the SAS motor in one of the mills [36].

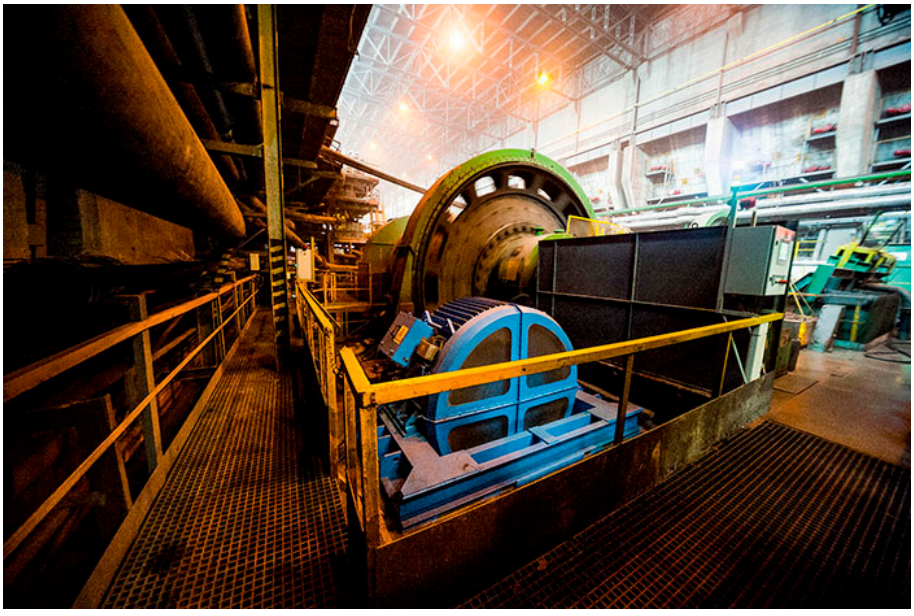

Figure 4. New ball mill drive system with the prototype energy-saving SMH motor [37].

As in the case of the SAS motor, the new drive system does not have a gearbox or a starter. The start of the charged ball mill is very violent, as shown in the graphs from the industrial HIOKI logger (Figure 5).

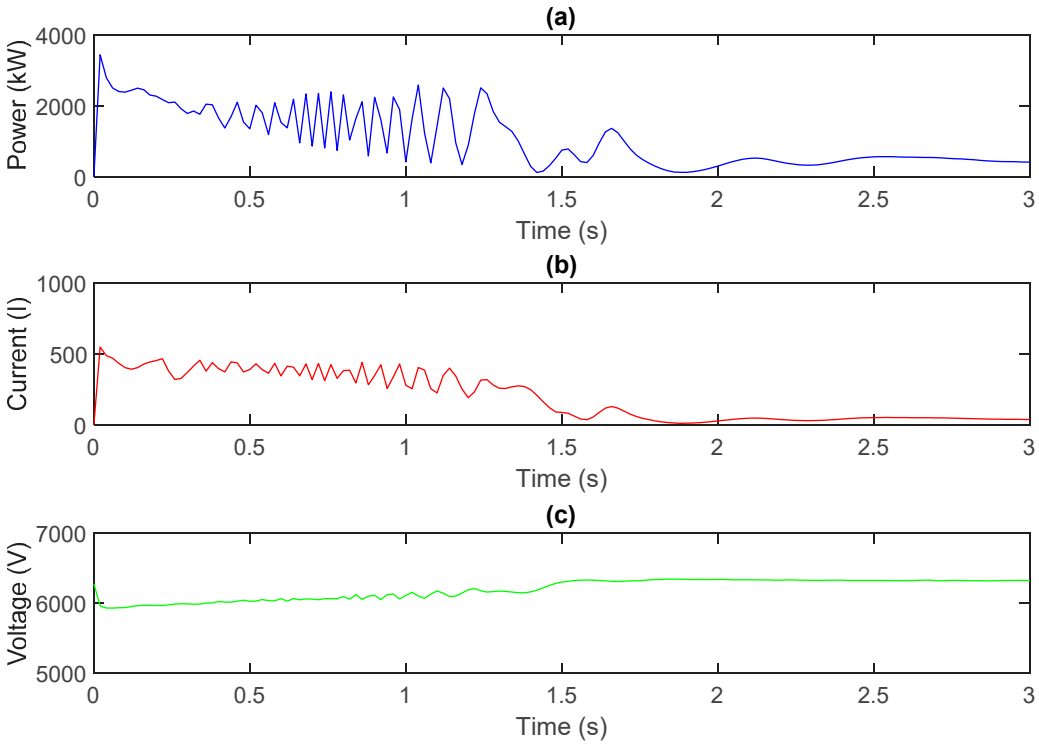

Figure 5. Start-up of the LSPMSM SMH-1732T motor with a filled ball mill after two hours of downtime: (**a**) active power, (**b**) current intensity, (**c**) voltage.

The start-up of the new motor lasts for approximately 2 s (Figure 5). Immediately after the motor starts, its instantaneous active power reaches the peak value of 3500 kW, being more than 5-fold in excess of its nominal power (Figure 5a). The start-up also entails significant changes of current intensity in the windings of the motor (Figure 5b). The highest current values of 550 A are observed in the initial phase of the start-up. This phenomenon is accompanied by a voltage drop at approximately 6% of the voltage in the power supply line (Figure 5c). High instantaneous values of the start-up current and of the active power, with a simultaneous voltage drop, pose a considerable risk and may lead to an overload in the power supply line [28]. The start-up of the motor is obstructed due to not only high mass moments of the mill inertia but also the braking torque from the permanent magnets within the entire range of revolutions, which is clearly seen in the graph representing the mechanical characteristic of the motor (Figure 6). The torque generated on the motor shaft is the result of the torque from the cage and of the braking torque from the permanent magnets (Figure 6a).

After a violent start-up of the motor, the recorded active power becomes stable at 430 kW (70% of the nominal motor power) (Figure 7). As in the case of the SAS motor, the active power was measured for a loaded mill operating at the nominal efficiency of 80 Mg/h. In this case, the fluctuations of the active power in steady motion (Figure 7) are decidedly lower than in the case of the SAS motor (Figure 3).

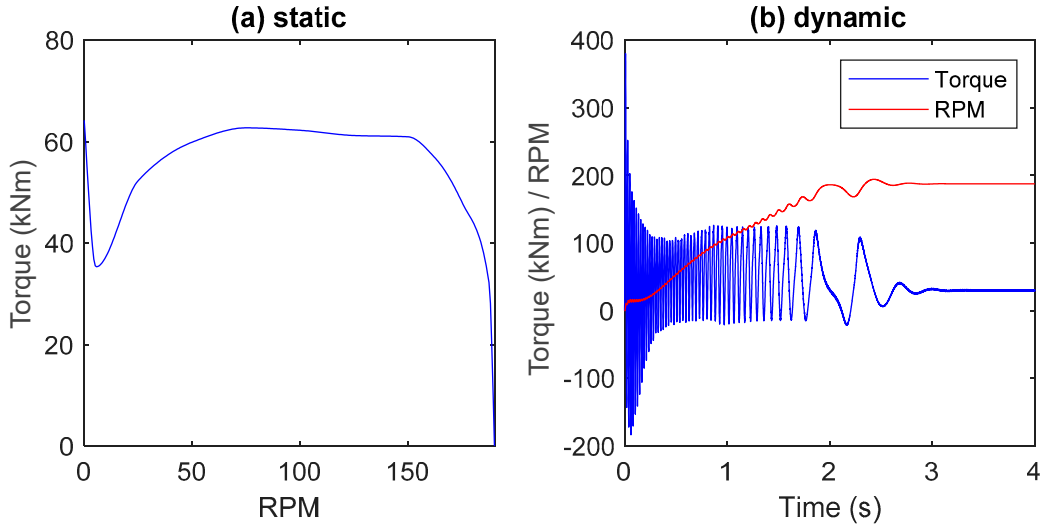

Figure 6. Mechanical characteristic of the LSPMSM SMH-1732T motor: (**a**) static, (**b**) dynamic [38].

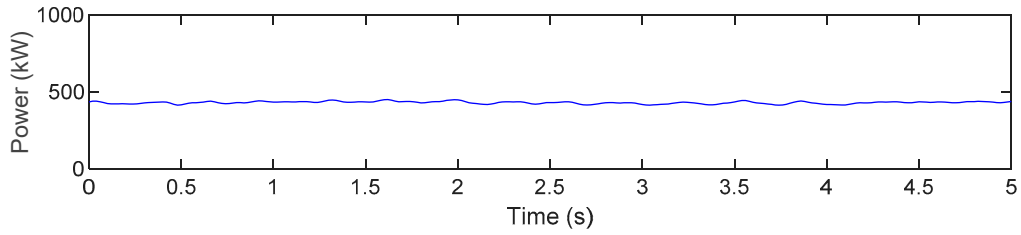

Figure 7. Active power of the LSPMSM SMH 1732T 630 kW motor during normal operation with filled ball mill.

One of the options for eliminating the problems related to the start-up process may be to implement a frequency converter in the power supply system [39,40], but a solution dedicated to this type of motors has not been developed yet.

3.3. Drive System with Asynchronous High-Efficiency Motor, with Gearbox, and with Fluid Coupling

Fluid coupling systems may be an alternative to expensive drive systems with frequency converters. Dynamic analyses demonstrated clearly that a fluid coupling may not be used in combination with a low-speed motor. The torque transmitted by a fluid coupling depends on the angular velocity of the input shaft and on the diameter of the shaft [40,41]. Thus, no coupling design exists that would enable transferring a torque of 32.1 kNm (the nominal torque of the SMH 630 kW motor) at 187.5 RPM (nominal revolutions of the SMH motor). The commercially available fluid couplings are used for revolutions above 700 RPM, with the torque increasing exponentially together with the increasing revolutions of the coupling [42]. Therefore, the use of fluid couplings is not possible in the above-described drive systems, both with the low-speed SAS and with the new SMH motors. For this reason, detailed consideration was given to the concept of a new drive system comprising a high-speed motor in a high-efficiency class (at least IE3), a gearbox, and a fluid coupling. The schematic diagram of the system is shown in Figure 8.

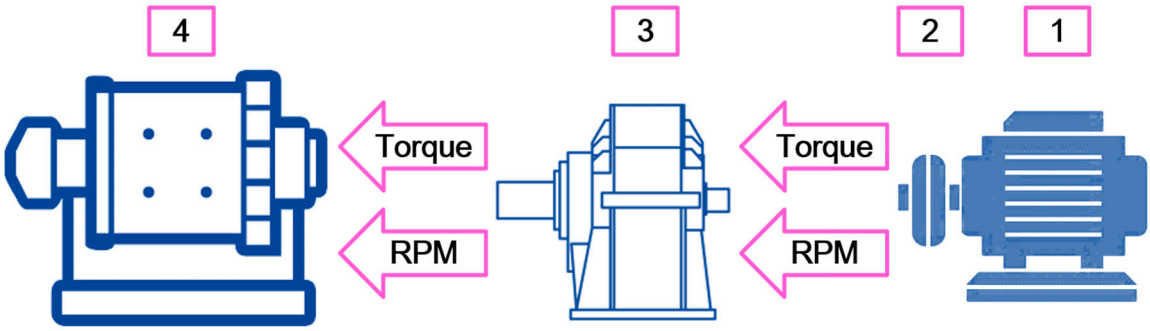

Figure 8. Schematic diagram of the drive system allowing the use of a fluid coupling for mill start-up: 1—asynchronous motor 630 kW 1000 RPM, 2—fluid coupling, 3—gearbox, 4—ball mill.

The electric motor used in this system had the same power as the motors used in the previous versions. The nominal revolutions of the motor are 1000 RPM. Therefore, an additional gearbox (3), with a 1:5 ratio, was required. The intermediate gearbox ensures optimum mill revolutions. The fluid coupling (2) was installed between the motor and the gearbox, on the high-speed shaft. Based on dynamic calculations, the selected coupling was TVV 866 with rotor diameter equal to 978 mm. Couplings of this type (TVV) are equipped with a delay chamber, which stores part of the fluid from the working circuit during downtime. A momentary decrease of the amount of fluid in the working circuit allows for more gentle torque behavior during the start-up. With time, the working fluid returns to the working circuit of the coupling, enabling it to transfer the nominal torque. The analysis of the new drive system was based on dynamic simulations of starting a mill fully charged with copper ore (Figure 9).

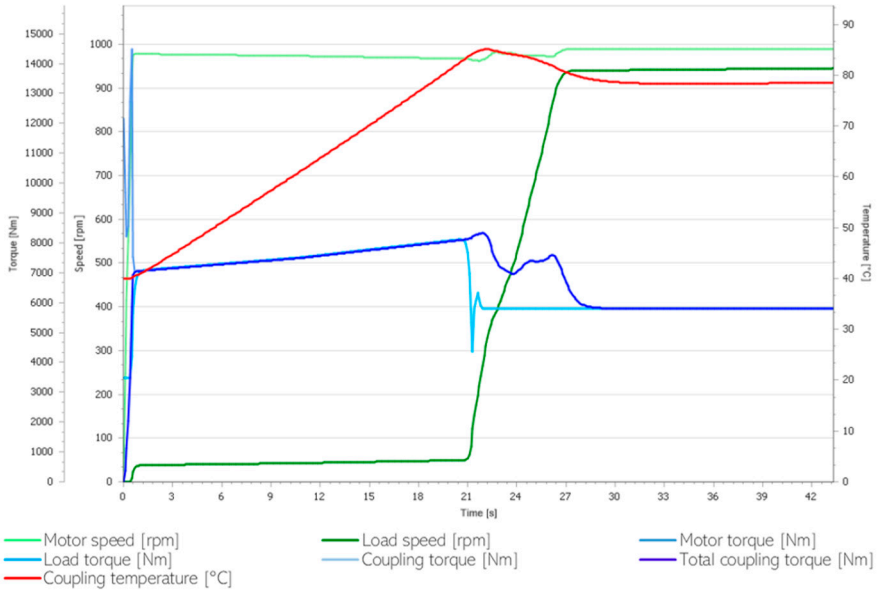

Figure 9. Dynamic simulation of the ball mill start-up process with the use of the TVV 866 fluid coupling.

The mill with the new drive system reaches the intended revolutions over a time of 27 s, and revolutions increase gently. This time duration can be thus assumed to be the mill start-up time proper. The final moment of the start-up process can be identified as the moment in which the motor starts to balance the anti-torque of the mill (power transmission). Both the entire torque transferred by the fluid coupling and the motor revolutions are stabilized. The working fluid used in the coupling is mineral oil, which reaches a maximum temperature of 85.1 °C after 21 s from the start-up. The working fluid temperature becomes stable at 79 °C after approximately 30 s. The coupling transfers a nominal torque of 5800 Nm

after 29 s and thus works in the medium load range. The nominal coupling slip in such conditions is 3.2%. In order to verify the thermal conditions, an additional simulation of two mill start-up processes was performed at short time intervals. The simulation results are shown in the graph below (Figure 10).

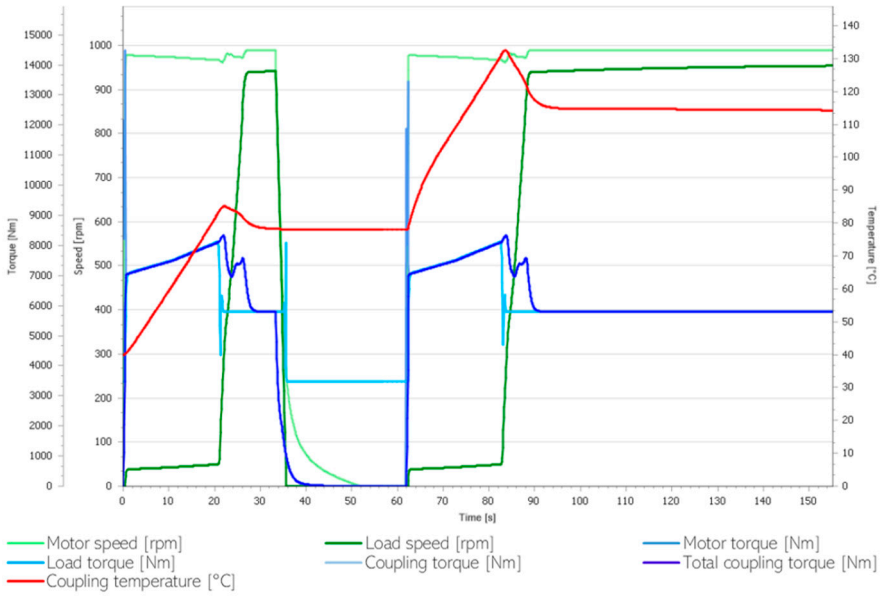

Figure 10. Dynamic simulation of two ball mill start-up processes with the use of the TVV 866 fluid coupling.

During the start-up, the energy transmission inside the coupling is the highest and results in an increased oil temperature. Performing two start-up processes over a short time period allows the assessment of both the maximum temperature increases and the cooling efficiency. Upon the second start-up, the maximum temperature of the working fluid momentarily reaches approximately 130 °C and then falls. The identified working temperatures of the coupling remain within the average range of loads and are thus safe for the drive system. The simulations were made for an engine with a rated power of 630 kW, operating with an effective power of 600 kW. The moment of inertia reduced to the motor shaft is 90.5 kgm^2 (the load torque reduced to the motor shaft is approx. 4600 Nm). The initial temperature was 40 °C.

4. Energy Efficiency Evaluation of the Analyzed Drive Systems

The simulations confirm that the application of a fluid coupling in the new drive system allows control of the ball mill start-up process. However, a complete analysis of each drive variant should also importantly involve the energy aspect. A reliable evaluation of the accuracy of the selected option must include an analysis and comparison of the energy efficiency of the drive systems. The comparison was based on two simple indicators. The first is the average electric energy consumption of the motor operating continuously for one hour. The second is the specific electric energy demand of the ball mill (i.e., the so-called specific energy consumption). This indicator defines the amount of electric energy required to process 1 Mg of copper ore. For this reason, it is strongly correlated with the first determined indicator. Note should be taken, however, that it does not allow for the quality-related parameters of the feed material and of the product (i.e., for the grain size composition).

This analysis was based on the measured electric energy consumption for the SAS and the SMH motors. With the known distributions of the ball mill operating parameters (efficiency and active power), the Monte Carlo method can be used to simulate the work areas in the analyzed variants. The simulation allows the expected energy consumption

variations to be represented in relation to the efficiency and enables an evaluation of the influence of these two parameters on the specific energy consumption. Both the instantaneous power of the drive system and the instantaneous efficiency of the ball mill were considered as input parameters for the simulation model. The model also allowed for the relationships between these parameters. The variability of the instantaneous drive system power was described on the basis of the measurement data. Table 1 shows the assumed variability parameters for the active power of the SAS motor (Variant 1) and of the SMH motor (Variant 2). The new system with the fluid coupling (Variant 3), which was not tested in actual operation, was described on the basis of the results obtained from the simulated start-up. In Variant 3, the motor with the nominal power of 630 kW was assumed to work at an average power of 600 kW.

Table 1. Statistical description of the active power values (in kW) used in the simulation.

No.	Parameter	Variant 1 (SAS)	Variant 2 (SMH)	Variant 3 (New Drive)
1	Average	601.77	429.75	600.04
2	Standard error	0.57	0.45	0.08
3	Standard deviation	29.68	7.74	1.43
4	Variance	880.93	59.84	2.04
5	Kurtosis	0.03	−0.20	−1.12
6	Skewness	0.50	−0.22	0.09

An important aspect of the simulation was to develop such a technological model of the operating ball mill that would allow for the energy consumption variability as a function of the production variability. The production variability allows for the random character of the feed stream (the ore fed to the mill) and for the variability of the output stream from the mill. Based on the measurement results, an assumption was made that the variability of the mill efficiency is ±5% of its nominal efficiency of 80 Mg/h. Figure 11 is a bar chart showing the probability distribution of ball mill efficiencies.

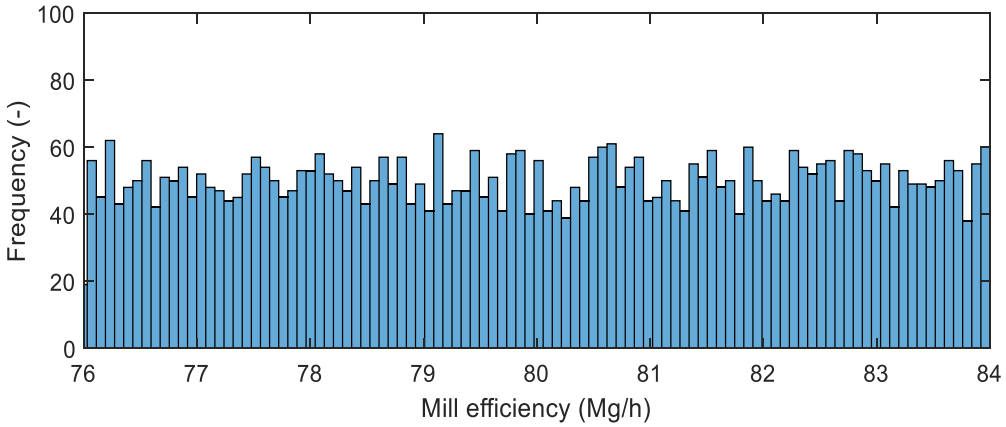

Figure 11. Bar chart of ball mill efficiencies (average value 80.02, standard error 0.033, standard deviation 2.32).

Figure 12 is a schematic diagram of the simulation algorithm. The output of the model provides statistically represented energy-consumption indicators.

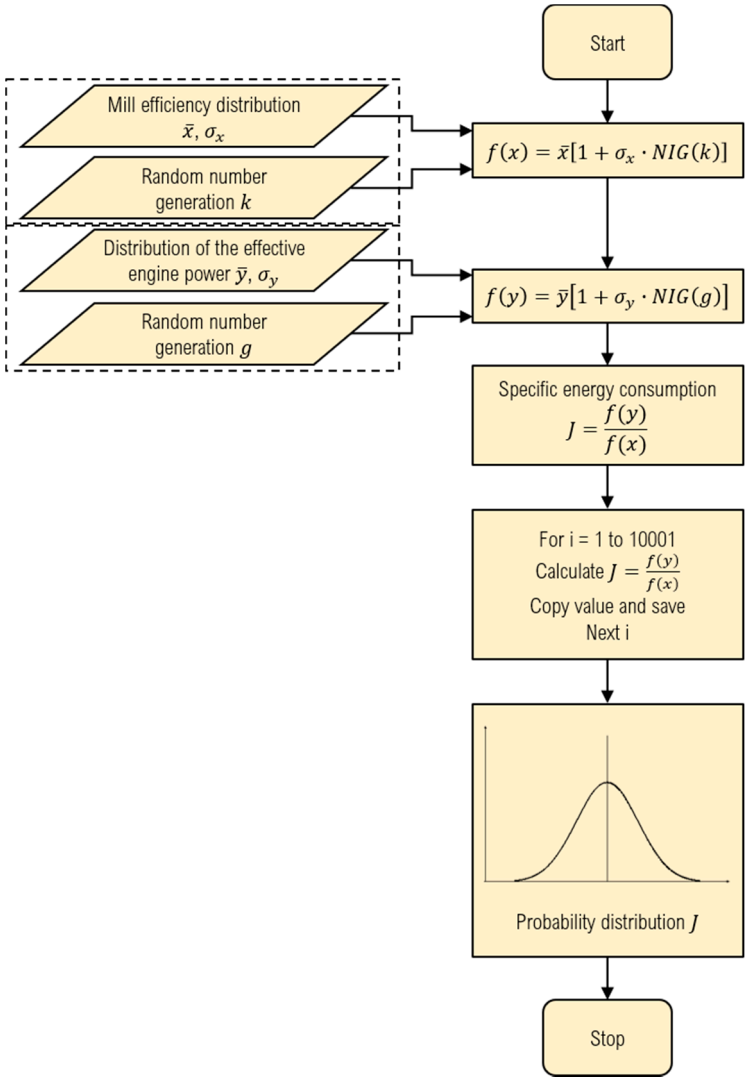

Figure 12. Algorithm of the Monte Carlo simulation.

The proper part of the Monte Carlo simulation consisted of 10,000 simulations, which served to calculate the variation range of the energy-consumption indicators. The random character of the process results in the formation of concentrated event areas (Figure 13a). Based on the statistical analysis, average points (Figure 13b) and specific energy consumption distributions (Figure 14) were identified for each drive variant.

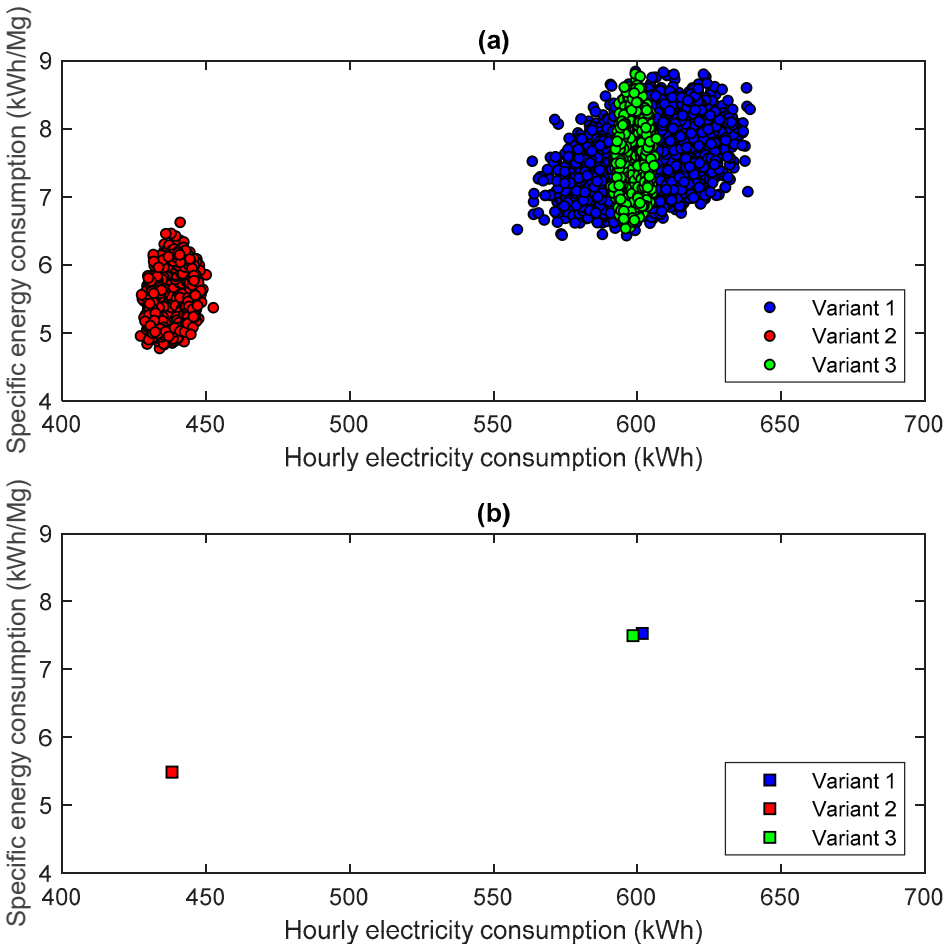

Figure 13. Monte Carlo simulation results—relationship between the specific energy consumption of the mill and the hourly electric energy consumption by a particular drive: (**a**) work areas of the selected drive systems, (**b**) averaged work points for Variant 1 (601.71 kWh; 7.53 kWh/Mg), Variant 2 (438.14 kWh; 5.49 kWh/Mg), and Variant 3 (598 46 kWh; 7.50 kWh/Mg).

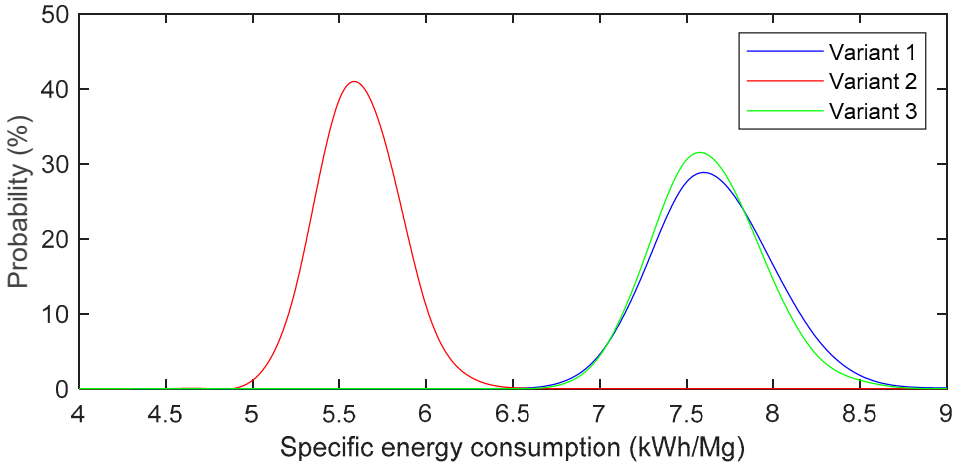

Figure 14. Probability distribution of specific energy consumption for the analyzed drive systems.

Tables 2 and 3 show statistical parameters characterizing the obtained indicators and values of simulation errors: MAE (mean absolute error) and RMSE (root mean squared error).

Table 2. Statistical description and errors of hourly electric energy consumption by each of the analyzed drives, obtained in Monte Carlo simulations. MAE: mean absolute error; RMSE: root mean squared error.

No.	Parameter	Variant 1 (SAS)	Variant 2 (SMH)	Variant 3 (New Drive)
1	Average	601.709	438.141	598.457
2	Standard deviation	10.823	3.038	1.993
3	Variance	117.143	9.231	3.974
4	Kurtosis	−0.012	0.042	0.041
5	Skewness	0.012	−0.011	0.034
6	MAE	8.642	2.408	1.585
7	RMSE	10.823	3.038	1.993

Table 3. Statistical description and errors of specific electric energy for each of the analyzed drives, obtained in Monte Carlo simulations.

No.	Parameter	Variant 1 (SAS)	Variant 2 (SMH)	Variant 3 (New Drive)
1	Average	7.530	5.489	7.496
2	Standard deviation	0.340	0.230	0.310
3	Variance	0.116	0.053	0.096
4	Kurtosis	0.030	0.129	0.101
5	Skewness	0.224	0.237	0.256
6	MAE	0.272	0.183	0.247
7	RMSE	0.340	0.230	0.310

5. Conclusions

The choice of a drive system for a ball mill used in copper ore comminution is largely dictated by the energy-related criteria. The energy efficiency of the three analyzed drives was identified in Monte Carlo simulations, which allow predictions of the most probable energy-consumption indicators. The research demonstrated that the old drive systems based on the SAS low-speed motors, which have been in operation for many years, have an average hourly electric energy consumption of 601.71 kWh and a specific energy consumption of 7.53 kWh/Mg. The replacement of the SAS motors with the new synchronous SMH motors induced with permanent magnets results in significant reductions of both the hourly energy consumption (to the level of 438.1 kWh) and the specific energy consumption (to the level of 5.49 kWh/Mg). The reduction in the energy consumption of the milling process is thus as much as 27%. The electricity demand indicators obtained by the simulation are in line with theoretical forecasts and measured values [12].

Solutions ensuring the gentle start-up of a mill filled to capacity are not available in the case of drive systems with low-speed SAS and SMH motors. The only solution seems to consist of pairing such motors with frequency converters. However, such solutions are not commercially available yet. An effective solution, which mitigates the problems related to the start-up process of a ball mill, can be provided by implementing asynchronous high-speed, high-efficiency motors. Based on the results of dynamic calculations, the new drive system design was paired with the TVV 866 fluid coupling. The simulated start-up process of the mill equipped with the new coupling demonstrated that this solution indeed allows for more gentle start-up behavior. As a result, the duration of the start-up process can be extended from 2 s (for the currently used drives) to 27 s. The analysis demonstrated that despite the two additional elements that affect the overall efficiency of the power transmission system (the gearbox and the fluid coupling), the energy-consumption indicators (the average, hourly electric energy consumption, and the specific energy consumption) remain slightly lower than in the traditional solution based on the SAS motor. The energy efficiency of this solution is much less advantageous than in the case of the SMH motor with permanent magnets. However, if compared with the traditional drives based on SAS motors (i.e., the drives to be replaced by the new solution), the average reduction in energy

consumption is 0.5%. Taking into perspective the scale of energy demand from the ore processing plant, the above difference allows an average daily savings of 78 kWh of electric energy to be obtained in the operation of a single mill. On an annual basis, this results in one mill providing more than 23 MWh of electric energy savings.

Taking into account only the energy-related criteria, the drive system with the SMH asynchronous permanent magnet motor seems to be the best solution. However, the choice of the drive system should also be dictated by economic criteria. If the operation of the drives with the SMH motors shows that the costs of their repairs due to overloads at start-up exceed the energy savings, then the solution with the fluid coupling may prove more advantageous.

Author Contributions: Conceptualization, methodology, software, and validation: M.O. and P.B.; writing—review, editing, and supervision: R.K. and L.G.; project administration: R.K. and L.G.; final text prepared by M.O., P.B., L.G. and R.K. All authors have read and agreed to the published version of the manuscript.

Funding: The research work was co-founded with the research subsidy of the Polish Ministry of Science and Higher Education granted for 2021.

Institutional Review Board Statement: Not applicable.

Data Availability Statement: The data presented in this study are available on request from the corresponding author.

Conflicts of Interest: The authors declare no conflict of interest.

References

1. Malinauskaite, J.; Jouhara, H.; Ahmad, L.; Milani, M.; Montorsi, L.; Venturelli, M. Energy efficiency in industry: EU and national policies in Italy and the UK. *Energy* **2019**, *172*, 255–269. [CrossRef]
2. Giridhar Kini, P.; Bansal, C.R. Energy Efficiency in Industrial Utilities. *Energy Manag. Syst.* **2011**. [CrossRef]
3. Kumar, A. Technomine, Mining Technology. Available online: http://technology.infomine.com/reviews/comminution/welcome.asp?view=full (accessed on 4 November 2020).
4. Jankovic, A.; Valery, W.; La Rosa, D. *Fine Grinding in the Australian Mining Industry*; Universiti Sains Malaysia: Nibong Tebal, Malaysia, 2008.
5. Jeswiet, J.; Szekeres, A. Energy Consumption in Mining Comminution. *Procedia CIRP* **2016**, *48*, 140–145. [CrossRef]
6. DOE. *Comminution and Energy Consumption: Report of the Committee on Comminution and Energy Consumption*; U.S. Department of Energy: Washington, DC, USA, 1981.
7. De Bakker, J. Energy Use of Fine Grinding in Mineral Processing. *Metall. Mater. Trans. E* **2014**, *1*, 8–19. [CrossRef]
8. Wojciechowski, B. Nie tylko wydobywamy. *Energetyka Cieplna i Zawodowa* **2015**, *2*, 20–23.
9. Rumpf, H. Problems of scientific development in particle technology, looked upon from a practical point of view. *Powder Technol.* **1977**, *18*, 3–17. [CrossRef]
10. Sidor, J. Directions in development of mills for raw materials and mineral binders grinding. *Mater. Ceram.* **2016**, *68*, 61–69.
11. Tamblyn, R.J. Analysis of Energy Requirements in Stirred Media Mills. Ph.D. Thesis, University of Birmingham, Birmingham, UK, 2009.
12. Krawczykowski, D.; Gawenda, T.; Foszcz, D. Comparison of real and theoretically estimated energy consumption for ball grinder. *Min. Geoengin.* **2006**, *30*, 79–90.
13. Wang, M.H.; Yang, R.Y.; Yu, A.B. DEM investigation of energy distribution and particle breakage in tumbling ball mills. *Powder Technol.* **2012**, *223*, 83–91. [CrossRef]
14. Mayank, K.; Malahe, M.; Govender, I.; Mangadoddy, N. Coupled DEM-CFD Model to Predict the Tumbling Mill Dynamics. *Procedia IUTAM* **2015**, *15*, 139–149. [CrossRef]
15. Marchal, G. Industrial experience with clinker grinding in the HOROMILL. In Proceedings of the IEEE Cement Industry Technical Conference (Paper), Hershey, PA, USA, 20–24 April 1997; pp. 195–211.
16. Tesema, G.; Worrell, E. Energy efficiency improvement potentials for the cement industry in Ethiopia. *Energy* **2015**, *93*, 2042–2052. [CrossRef]
17. Telichenko, V.I.; Sharapov, R.R.; Lozovaya, S.Y.; Skel, V.I. Analysis of the efficiency of the grinding process in closed circuit ball mills. In Proceedings of the MATEC Web of Conferences, EDP Sciences, Amsterdam, The Netherlands, 23–25 March 2016; Volume 86, p. 4040.
18. Rowland, C.A.; Erickson, M.T. Large Ball Mill Scale-Up Factors to Be Studied Relative to Grinding Efficiency. *Miner. Metall. Process.* **1984**, *1*, 165–172. [CrossRef]

19. Fuerstenau, D.W.; Lutch, J.J.; De, A. The effect of ball size on the energy efficiency of hybrid high-pressure roll mill/ball mill grinding. *Powder Technol.* **1999**, *105*, 199–204. [CrossRef]
20. Zheng, J.; Harris, C.C.; Somasundaran, P. A study on grinding and energy input in stirred media mills. *Powder Technol.* **1996**, *86*, 171–178. [CrossRef]
21. Costea, C.; Silaghi, H.; Silaghi, M.; Silaghi, P. Mill speed control using programmable logic controllers. In Proceedings of the International Conference on Mathematical Methods and Computational Techniques in Electrical Engineering, Timișoara, Romania, 21–23 October 2010; World Scientific and Engineering Academy and Society (WSEAS): Stevens Point, WI, USA, 2010; pp. 26–30, ISBN 978-960-6766-60-2.
22. El-Shall, H.; Somasundaran, P. Physico-chemical aspects of grinding: A review of use of additives. *Powder Technol.* **1984**, *38*, 275–293. [CrossRef]
23. Pacholski, E.; Iskierski, L. The analisis of influence of start-up mode of drive motors to electric network parameters. *Electr. Mach. Trans. J.* **2013**, *2*, 99.
24. Bianchi, N.; Bolognani, S.; Frare, P. Design criteria for high-efficiency SPM synchronous motors. *IEEE Trans. Energy Convers.* **2006**, *21*, 396–404. [CrossRef]
25. Lu, X.; Iyer, K.L.V.; Mukherjee, K.; Kar, N.C. Development of a novel magnetic circuit model for design of premium efficiency three-phase line start permanent magnet machines with improved starting performance. *IEEE Trans. Magn.* **2013**, *49*, 3965–3968. [CrossRef]
26. Stoia, D.; Chirilă, O.; Cernat, M.; Hameyer, K.; Ban, D. The behaviour of the LSPMSM in asynchronous operation. In Proceedings of the EPE-PEMC 2010—14th International Power Electronics and Motion Control Conference, Ohrid, North Macedonia, 6–8 September 2010; pp. T4–T45.
27. Mayer, C.B.; Johnson, R.M.; Gray, D.J. Solution of a Serious Repetitive Vibration Problem on a 4500-hp Single-Pinion Synchronous Motor Ball Mill Drive. *IEEE Trans. Ind. Appl.* **1985**, *IA-21*, 1039–1046. [CrossRef]
28. Zawilak, T.; Zawilak, J. Energy-efficient motor in ball mill applcation. *Drives Control* **2017**, *19*, 68–72.
29. Gao, X.; Wang, X.; Wei, Z. Design and control of high-capacity and lowspeed doubly fed start-up permanent magnet synchronous motor. *IET Electr. Power Appl.* **2018**, *12*, 1350–1356. [CrossRef]
30. Mirošević, M.; Maljković, Z. Effect of sudden change load on isolated electrical grid. In Proceedings of the Electrical Systems for Aircraft, Railway and Ship Propulsion, ESARS, Aachen, Germany, 3–5 March 2015; pp. 1–4.
31. McElveen, R.F.; Toney, M.K. Starting high-inertia loads. *IEEE Trans. Ind. Appl.* **2001**, *37*, 137–144. [CrossRef]
32. Leng, S.; Ul Haque, A.R.N.M.R.; Perera, N.; Knight, A.; Salmon, J. Soft Start and Voltage Control of Induction Motors Using Floating Capacitor H-Bridge Converters. *IEEE Trans. Ind. Appl.* **2016**, *52*, 3115–3123. [CrossRef]
33. Zenginobuz, G.; Çadirci, I.; Ermiş, M.; Barlak, C. Soft starting of large induction motors at constant current with minimized starting torque pulsations. *IEEE Trans. Ind. Appl.* **2001**, *37*, 1334–1347. [CrossRef]
34. Pacholski, E.; Leśnik, M. Sas motors exploitation in kghm polska miedz s.a. division of concentrator. Experience, problems, priority activities. *Electr. Mach. Trans. J.* **2012**, *1*, 153–157.
35. Zawilak, T. Synchronous motors excited by permanent magnets in high power drives. *Przegląd Elektrotechniczny* **2017**, *1*, 175–178. [CrossRef]
36. Kisielewski, P.; Leśnik, M.; Pacholski, E.; Zawilak, J.; Zawilak, T. Design, construction and testing of prototypes series of large synchronous motors with permanent magnets. *Electr. Mach. Trans. J.* **2016**, *3*, 191–195.
37. KGHM Polska Miedź S.A. *Promotional Materials*; KGHM Polska Miedź S.A.: Lubin, Poland, 2020.
38. Start, L.; Magnet, P.; Motor, S.; Ball, I.N. Line start permanent magnet synchronous motor in ball mill application. *Electr. Mach. Trans. J.* **2016**, *2016*, 169–173.
39. Ni, R.; Xu, D.; Blaabjerg, F.; Wang, G.; Li, B.; Lu, K. Synchronous switching of non-line-start permanent magnet synchronous machines between inverter and grid drives. In Proceedings of the 2016 IEEE Energy Conversion Congress and Exposition (ECCE), Milwaukee, WI, USA, 18–22 September 2016; Volume 31, pp. 3717–3727. [CrossRef]
40. Brun, K.; Meyenberg, C.; Thorp, J. Hydrodynamic torque converters for oil & gas compression and pumping applications: Basc principles, performance characteristics and applications. In Proceedings of the Asia Turbomachinery & Pump Symposium, Singapore, 22–25 February 2016; Turbomachinery Laboratories, Texas A&M Engineering Experiment Station: College Station, TX, USA, 2016; p. 15.
41. Heisler, H. Hydrokinetic fluid couplings and torque converters. In *Advanced Vehicle Technology*; Elsevier: Amsterdam, The Netherlands, 2002; pp. 98–116. ISBN 9780750651318.
42. Huitenga, H.; Mitra, N.K. Improving startup behavior of fluid couplings through modification of runner geometry: Part I—Fluid flow analysis and proposed improvement. *J. Fluids Eng. Trans. ASME* **2000**, *122*, 689–693. [CrossRef]